Structural Variances in the Homologous Series of Di-Alkali-Metalated Octamethylcyclotetrasilazanes

Thomas Kottke and Dietmar Stalke*

Institut für Anorganische Chemie der Universität Würzburg, Am Hubland, D-97074 Würzburg, Germany

Received June 3, 1996[⊗]

The rubidium and cesium dimetalated derivatives of octamethylcyclotetrasilazane (OMCTS) have been synthesized and crystallographically characterized. This completes the set of di-alkali-metalated OMCTS structures. Comparison of the geometric parameters within the series reveals the cation-induced alterations of coordination and aggregation as well as of bonding within, and conformation of, the anionic fragment. With the increasing size and the decreasing charge-localizing effect of the cation going from lithium to cesium, the coordination number and "haptotropicity" of the cation systematically increases, while the preference of the deprotonated nitrogen atoms over the N(H) functional nitrogen atoms for an electrostatic interaction decreases in this order. At the same time, the distortion of the ring geometry caused by the charge-localizing effect of the cation decreases such that the anionic fragment approaches the symmetric crown conformation. Within the ring system, the character of the Si−N bond becomes more ionic, which explains the increasing deviation of short and long Si−N bond lengths. That properties for a certain species are still not entirely deducible from respective data of homologous compounds is revealed by unexpected inconsistencies within the structural and chemical characteristics of the compounds investigated. For instance, the dimeric aggregation of the potassium compound contrasts with the polymeric form of the rubidium and cesium structures despite the close relationship between these metals. Moreover, the course of reactivity of the elemental alkali metals with respect to the deprotonation of OMCTS seems to conflict with their reduction potentials but can be explained by considering the steric situation at the N(H) active site of the precursor.

Introduction

Since the discovery of alkyllithium compounds by Schlenk and Holtz in 1917,[1] studies of the application of organo-alkali metal reagents in synthetic chemistry focused on lithium species, as documented by the comprehensive literature available in this area.[2] High regioselectivity, excellent solubility even in nonpolar solvents, and industrial synthesis and application are factors which contributed to the preference for organolithium compounds over related derivatives of the heavier alkali metals. Initiated by the fundamental work by Lochmann and Schlosser in the late 1960s,[3] the use of heavier group 1 organometallic compounds in preparative chemistry experienced a renaissance with the introduction of the so-called superbasic mixtures. Ever since, several studies illustrated the often entirely different reaction behavior within group 1 organometallics,[2c,4] and it is a subject of current interest to determine the parameters governing this variance.[5]

The structural investigation of a complete homologous series of alkali metalated derivatives provides a promising approach to address this question. Thereby, information about the geometrical effects caused by the variation of the metal cation can be obtained. A direct comparison, however, requires minimizing nonrelated effects which may arise when different solvents or substituents are employed. So far, only a few systems featuring the complete set of cations from lithium to cesium have been crystallographically characterized. Examples are the alkali-metalated derivatives of methane[6] (analyzed by powder diffraction), triphenylmethane,[7] carbazole,[8] iminosulfinamine,[9] aminoiminophosphorane,[10] and bis(trimethylsilyl)amine,[11] most of which contain varying substituents or ligands. Some general trends are nevertheless apparent and can be attributed

[⊗] Abstract published in *Advance ACS Abstracts,* September 15, 1996.

(1) (1) Schlenk, W.; Holtz, J. *Ber. Dtsch. Chem. Ges.* **1917**, *50*, 262.

(2) (a) Wakefield, B. J. *Organolithium Compounds*; Pergamon Press: Oxford, 1974. (b) Wilkinson, G., Stone, F. G. A., Abel, E. W., Eds. *Comprehensive Organometallic Chemistry*; Pergamon Press: Oxford, 1982; Vol. 1. (c) Brandsma, L.; Verkruijsse, H. *Preparative Polar Organometallic Chemistry*; Springer-Verlag: Berlin, 1987; Vol. 1. (d) Maercker, A. *Top. Curr. Chem.* **1987**, *138*, 1. (e) Wakefield, B. J. *Organolithium Methods*; Academic Press: London, 1988. (f) Brandsma, L. *Preparative Polar Organometallic Chemistry*; Springer-Verlag: Berlin, 1990; Vol. 2. (g) Snieckus, V. *Chem. Rev.* **1990**, *90*, 879. (h) Sapse, A.-M., Schleyer, P. v. R., Eds. *Lithium Chemistry*; John Wiley & Sons: New York, 1994. (i) Snaith, R., Ed. *Chemistry of the Alkali and Alkaline Earth Metals*; VCH, Weinheim: in press.

(3) (a) Lochmann, L.; Pospisil, J.; Lim, D. *Tetrahedron Lett.* **1966**, 257. (b) Schlosser, M. J. *J. Organomet. Chem.* **1967**, *8*, 9.

(4) (a) Schlosser, M. *Struktur und Reaktivität polarer Organometalle*; Springer: Berlin, 1973; p 147. (b) Schlosser, M. In *Modern Synthetic Methods; Scheffold, R., Ed.;* Helvetica Chimica Acta: Basel, 1992; Vol. 6, p 227. (c) Mordini, A. In *Advances in Carbanion Chemistry;* Snieckus, V., Ed.; Jai Press: London, 1992; Vol. 1, p1. (d) Gornitzka, H.; Stalke, D. *Angew. Chem.* **1994**, *106*, 695; *Angew. Chem., Int. Ed. Engl.* **1994**, *33*, 693; *Organometallics* **1994**, *13*, 4398.

(5) Lambert, C.; Schleyer, P. v. R. *Angew. Chem.* **1994**, *106*, 1187; *Angew. Chem., Int. Ed. Engl.* **1994**, *33*, 1129.

(6) Weiss, E. *Angew. Chem.* **1993**, *105*, 1565; *Angew. Chem., Int. Ed. Engl.* **1993**, *32*, 1501.

(7) (a) Brooks, J. J.; Stucky, G. D. *J. Am. Chem. Soc.* **1972**, *94*, 7333. (b) Köster, H.; Weiss, E. *J. Organomet. Chem.* **1979**, *168*, 273. (c) Olmstead, M. M.; Power, P. P. *J. Am. Chem. Soc.* **1985**, *107*, 2174. (d) Bartlett, R. A.; Dias, H. v. R.; Power, P. P. *J. Organomet. Chem.* **1988**, *341*, 1. (e) Hoffmann, D.; Bauer, W.; Schleyer, P. v. R.; Pieper, U.; Stalke, D. *Organometallics* **1993**, *12*, 1193.

S0276-7333(96)00434-7 CCC: $12.00

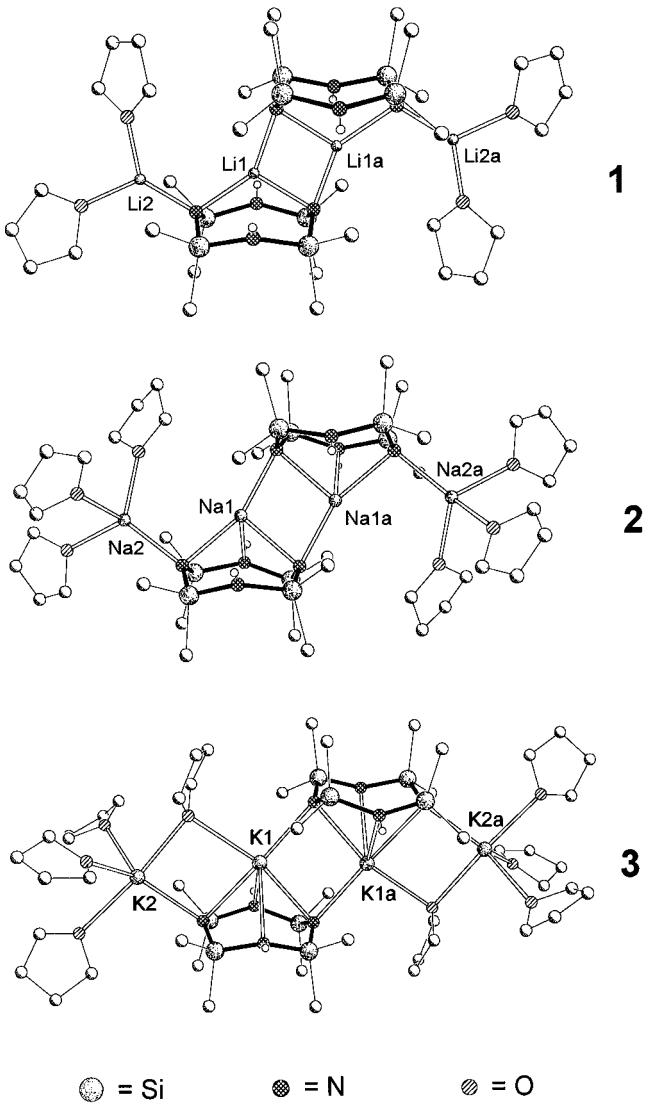

Figure 1. Dimeric structures of $[Li_2(Me_2SiN(H)Me_2SiN)_2 \cdot 2THF]_2$ (**1**), $[Na_2(Me_2SiN(H)Me_2SiN)_2 \cdot 3THF]_2$ (**2**), and $[K_2(Me_2SiN(H)Me_2SiN)_2 \cdot 4THF]_2$ (**3**) in the crystal.[13]

essentially to the different cation sizes. Not surprisingly, a higher degree of association along with an increased coordination number of the respective cation is characteristic, going from lithium to cesium. In π-delocalized carbanionic systems multihapto bonding prevails for the heavier alkali metals due to their lesser charge-localizing effect.[7e] However, if heteroatoms are part of the anionic moieties a coordinative position at the negatively charged heteroatom is preferred as exemplified by the structures of alkali-metalated diphenylpyridylmethane.[12] Some modifications in the anion have been detected, as well. For instance, the pyramidalization of the deprotonated carbon atom in the Ph_3C^- system vanishes with increasing cation size, reflecting more ionic geometries in the derivatives of the heavier alkali metals.[7e]

Herein we present the solid-state structures of rubidium (**4**) and cesium (**5**) dimetalated octamethylcyclotetrasilazane (OMCTS) which complete the set of related alkali-metal structures previously determined (Figure 1).[13] All compounds were investigated under the same conditions (THF as the polar ligand, low-temperature structure determination) which allows us not only to directly correlate the coordination differences with the characteristics of the corresponding alkali metals but also to uncover marginal variances within the anion.

Results and Discussion

Differences within the group of alkali metals already occur in the deprotonation reaction of OMCTS. While *n*-BuLi is used to prepare the lithium compound $[Li_2\{Si(Me_2)N(H)Si(Me_2)N\}_2 \cdot 2THF]_2$ (**1**),[13a] elemental sodium, potassium, and rubidium are sufficiently reactive to convert the cyclotetrasilazane into the metalated derivatives $[Na_2\{Si(Me_2)N(H)Si(Me_2)N\}_2 \cdot 3THF]_2$ (**2**),[13b] $[K_2\{Si(Me_2)N(H)Si(Me_2)N\}_2 \cdot 4THF]_2$ (**3**),[13b] and $[Rb_2\{Si(Me_2)N(H)Si(Me_2)N\}_2 \cdot 3THF]_\infty$ (**4**), (eq 1). In the latter

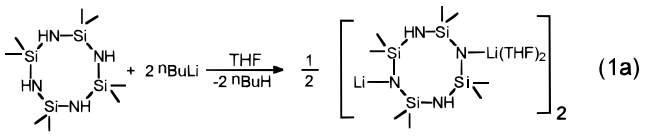

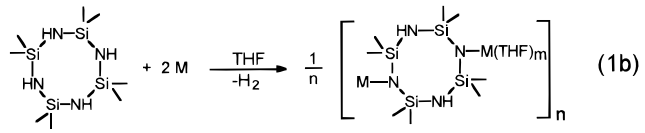

2: M = Na; m = 3; n = 2
3: M = K; m = 4; n = 2
4: M = Rb; m = 3; n = ∞

case, comparatively drastic conditions were necessary to force conversion. During the reaction time of 3 days the rubidium metal had to be activated by ultrasound in refluxing THF and finely dispersed by employing a mechanical disintegrater. In contrast to Na, K, and Rb, cesium metal does not deprotonate the silazane directly. A straightforward reaction, however, can be achieved with the use of catalytic amounts of toluene which leads to the intermediate formation of benzylcesium. In the second step, the benzyl anion deprotonates OMCTS in

(8) (a) Hacker, R.; Kaufmann, E.; Schleyer, P. v. R.; Mahdi, W.; Dietrich, H. *Chem. Ber.* **1987**, *120*, 1533. (b) Gregory, K.; Bremer, M.; Schleyer, P. v. R.; Klusener, P. A. A.; Brandsma, L. *Angew. Chem.* **1989**, *101*, 1261; *Angew. Chem. Int. Ed. Engl.* **1989**, *28*, 1224. (c) Gregory, K. Ph.D. thesis, University of Erlangen-Nürnberg, 1991.

(9) (a) Pauer, F.; Stalke, D. *J. Organomet. Chem.* **1991**, *418*, 127. (b) Edelmann, F. T.; Knösel, F.; Pauer, F.; Stalke, D.; Bauer, W. *J. Organomet. Chem.* **1992**, *438*, 1. (c) Freitag, S.; Kolodziejski, W.; Pauer, F.; Stalke, D. *J. Chem. Soc., Dalton Trans.* **1993**, 3479.

(10) Steiner, A.; Stalke, D. *Inorg. Chem.* **1993**, *32*, 1977.

(11) (a) Domingos, A. M.; Sheldrick, G. M. *Acta Crystallogr.* **1974**, *B30*, 517. (b) Engelhardt, L. M.; May, A. S.; Raston, C.; White, A. H. *J. Chem. Soc., Dalton Trans.* **1983**, 1671. (c) Lappert, M. F.; Slade, M. J.; Singh, A.; Atwood, J. L.; Rogers, R. D.; Shakir, R. *J. Am. Chem. Soc.* **1983**, *105*, 302. (d) Power, P. P.; Xiaojie, X. J. *J. Chem. Soc., Chem. Commun.* **1984**, 358. (e) Engelhardt, L. M.; Jolly, B. S.; Junk, P. C.; Raston, C. L.; Skelton, B. W.; White, A. H. *Aust. J. Chem.* **1986**, *39*, 1337. (f) Williard, P. G. *Acta Crystallogr.* **1988**, *C44*, 270. (g) Edelmann, F. T.; Pauer, F.; Wedler, M.; Stalke, D. *Inorg. Chem.* **1992**, *31*, 4143. (h) Williard, P. G.; Liu, Q.-Y., Lochmann, L. *J. Am. Chem. Soc.* **1992**, *114*, 348.

(12) Pieper, U.; Stalke, D. *Organometallics* **1993**, *12*, 1201.

(13) (a) Dippel, K.; Klingebiel, U.; Noltemeyer, M.; Pauer, F.; Sheldrick, G. M. *Angew. Chem.* **1988**, *100*, 1093; *Angew. Chem., Int. Ed. Engl.* **1988**, *27*, 1074. (b) Dippel, K.; Klingebiel, U.; Kottke, T.; Pauer, F.; Sheldrick, G. M.; Stalke, D. *Chem. Ber.* **1990**, *123*, 237.

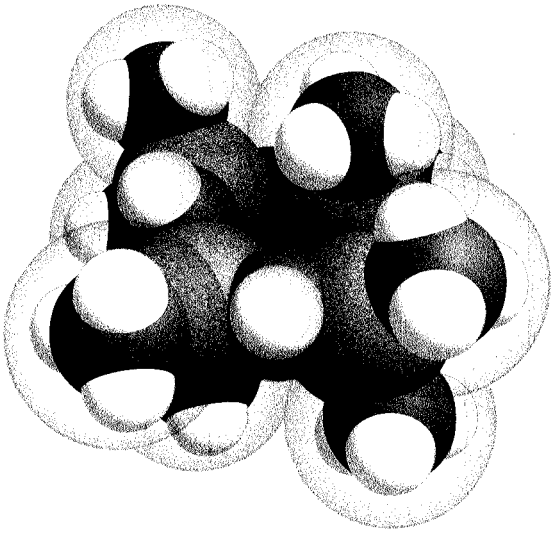

Figure 2. Space filling model of the molecular structure of OMCTS in its crown conformation. The methyl groups have been overlaid by their van der Waals spheres illustrating the sterical shielding of the N(H) function.

a one-phase reaction affording the cesium compound **5** and toluene (eq 2).

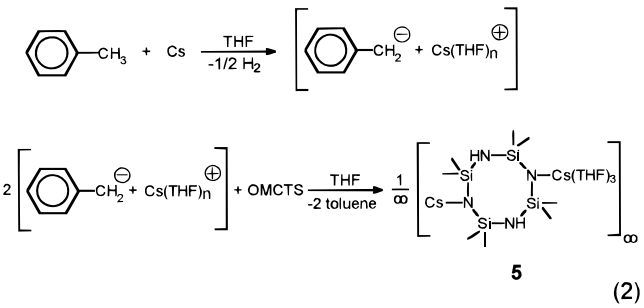

5 (2)

The course of reactivity of the alkali metals toward OMCTS is fairly unusual as it does not correspond with the reduction potentials. The low reactivity of elementary rubidium and the inert behavior of cesium, in particular, implies that geometrical aspects have to be considered, as well. A space-filling representation of nonmetalated OMCTS in its crown conformation[14] illustrates the steric situation at the N−H active site (Figure 2). On the basis of the sum of the covalent radii[15] of carbon and hydrogen (1.4 Å) on the one hand and the van der Waals radius[15] of a methyl group (2.0 Å) on the other hand, the gap between the two methyl groups "framing" the N−H fragment should be within the range of 1.5−2.7 Å (rotation of the methyl group allowed). For comparison, the atomic radii of the alkali metals[16] are 1.52 (Li), 1.86 (Na), 2.27 (K), 2.48 (Rb), and 2.65 Å (Cs). Apparently, an attack of the N−H function by the comparatively large cesium atom is sterically hindered by the ligands in neighboring positions.

Solid-State Structure of $[Rb_2(Me_2SiN(H)Me_2SiN)_2 \cdot 3THF]_\infty$ (4). In contrast to the dimeric structures of Li, Na, and K dimetalated OMCTS, the rubidium derivative **4** forms a polymeric chain in the solid state (Figure 3). Electrostatic interactions with the eight-membered SiN ring, which approximates a crown conformation, and with the THF molecules result in rubidium being 4- and 7-fold coordinated, respectively. Geometrical information is contained in Table 1.

The anionic moieties are connected via terminally arranged rubidium atoms (Rb2 and Rb3), each of which is coordinated by two μ_2-bridging THF molecules and two deprotonated nitrogen atoms. Crystallographically, Rb2 and Rb3 are located at two centers of inversion inducing the one-dimensional infinite association of the monomeric units. As a consequence, the terminal rubidium atoms show planar coordination, and the distances to the deprotonated nitrogen atoms of both connected silazane rings are equivalent by means of symmetry, as are the Rb−O distances to the attached THF molecules. The third rubidium atom in the asymmetric unit is positioned almost centrally above the eight-membered ring; the projection onto the averaged ring plane deviates by only 0.052 Å (corresponding to 2.5% of the average ring radius) from the calculated center. As a consequence, four Rb−N contacts are formed at one side of the metal hemisphere while three THF molecules, two of which are μ_2-bridging the terminal Rb atoms, complete the coordination sphere from the opposite side (Figure 4).

The distances of Rb1 to the deprotonated nitrogen atoms N1 and N3 (2.957(4) and 2.987(4) Å) are almost 0.2 Å shorter than to the N(H) functional nitrogen atoms N2 and N4 (3.161(5) and 3.138(5) Å). At the same time, the Si−N−Si bond angles are slightly larger at N1 and N3 (140.4(3) and 136.5(2)°) than at N2 and N4 (131.0(3) and 130.9(2)°), reflecting the deformation of the ring system. The distances across the ring may serve as an additional probe for this distortion. The vector N1···N3 (3.811 Å) is significantly shorter than N2···N4 (4.240 Å) which illustrates a contraction of the ring along the line N1···N3, i.e., the eight-membered ring is squeezed together by the electrostatic attraction between the negatively charged deprotonated nitrogen atoms and the rubidium cation. In connection with this, the endocyclic ring angles at N1 and N3 open in order to account for the increased steric strain as revealed by comparison with the endocyclic angles at the N(H) functional nitrogen atoms. The variation of the distances and angles within the ring framework can be attributed to polarity differences of the Si−N bonds. The negative charge at the deprotonated nitrogen atoms increases the ionic character of the Si−N bonds and a bond shortening results.

The rubidium atoms in terminal position form slightly shorter distances to the deprotonated nitrogen atoms than the cations arranged centrally above the silazane ring (Rb2−N1 = 2.911(4) and Rb3−N3 = 2.875(4) Å vs Rb1−N1 = 2.957(4) and Rb1−N3 = 2.987(4) Å) which compensates for their lower coordination number. In fact, the shorter Rb−N distances rank at the lower limit of the usual range observed in organometallic compounds containing Rb−N contacts (2.92−3.25 Å from 13 entries in the CSD[17]). Marginal variances in the Rb−O distances reflect the different coordination mode of the THF molecules with respect to terminal and μ_2-coordination (Rb1−O2 = 2.938(5) Å; Rb−O of bridging THF, 2.993(4)−3.088(5) Å). Although, bridging coordi-

(14) Smith, G. S.; Alexander, L. E. *Acta Crystallogr.* **1963**, *16*, 1015.
(15) Pauling, L. *The Nature of the Chemical Bond*; Cornell University Press: Ithaca, NY, 1960.
(16) Emsley, J. *The Elements*; Clarendon Press: Oxford, 1991.
(17) Allen, F. H.; Kennard, O. *Chem. Des. Automation News* **1993**, *8*, 131.

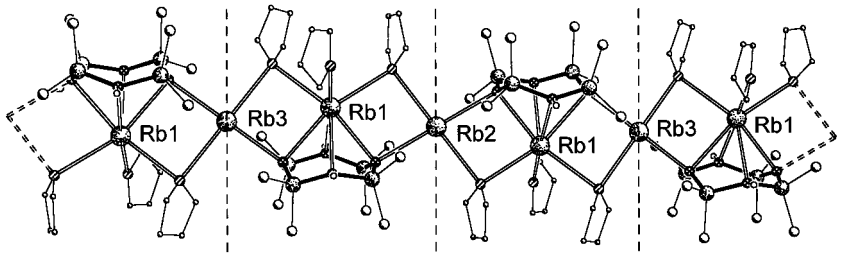

Figure 3. Polymeric structure of $[Rb_2(Me_2SiN(H)Me_2SiN)_2 \cdot 3THF]_\infty$ (**4**) in the crystal (Rb2 and Rb3 are on special positions).

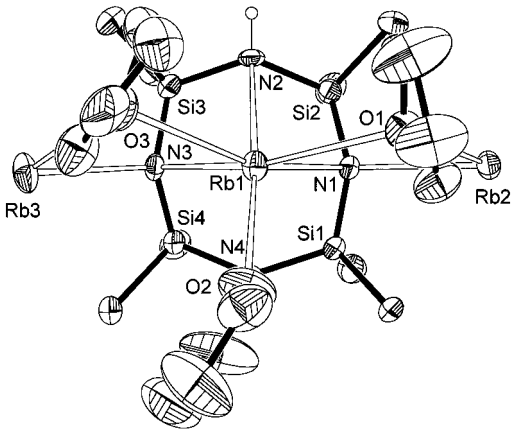

Figure 4. Asymmetric unit of **4** without H(C) atoms; anisotropic uncertainty parameters depicting 50% probability.

Table 1. Selected Bond Lengths (Å) and Angles (deg) of 4 and 5

4		5	
Rb1−N1	2.957(4)	Cs1−N1	3.207(3)
Rb1−N2	3.161(5)	Cs1−N2	3.351(3)
Rb1−N3	2.987(4)	Cs1−N3	3.125(3)
Rb1−N4	3.138(5)	Cs1−N4	3.393(3)
Rb1−O1	3.021(4)	Cs1−O1	3.207(3)
Rb1−O2	2.938(5)	Cs1−O2	3.340(3)
Rb1−O3	3.042(4)	Cs2−N1	3.133(3)
Rb2−N1	2.911(4)	Cs2−O1	3.379(3)
Rb2−O1	2.993(4)	Cs2−O2	3.216(3)
Rb3−N3	2.875(4)	Cs2−O3	3.193(2)
Rb3−O3	3.088(5)	Cs2−N3a	3.076(2)
Si1−N1	1.655(5)	Si1−N1	1.669(3)
Si2−N1	1.658(4)	Si2−N1	1.662(3)
Si2−N2	1.757(4)	Si2−N2	1.754(3)
Si3−N2	1.748(4)	Si3−N2	1.752(3)
Si3−N3	1.672(4)	Si3−N3	1.660(3)
Si4−N3	1.652(4)	Si4−N3	1.667(3)
Si4−N4	1.749(4)	Si4−N4	1.756(3)
Si1−N4	1.752(4)	Si1−N4	1.747(3)
N1−Rb1−N3	79.76(12)	N1−Cs1−N3	74.86(6)
N2−Rb1−N4	84.61(12)	N2−Cs1−N4	77.68(7)
O1−Rb1−O3	109.23(12)	O1−Cs1−O2	72.38(7)
N1−Rb2−O1	82.28(11)	N1−Cs2−N3a	110.62(7)
N3−Rb3−O3	85.64(12)	N1−Cs2−O3	163.62(6)
Rb1−O1−Rb2	95.71(12)	Cs1−O1−Cs2	78.32(6)
Rb1−O3−Rb3	88.49(11)	Cs1−O2−Cs2	78.79(6)
Si1−N1−Si2	140.4(3)	Si1−N1−Si2	133.0(2)
Si2−N2−Si3	131.0(3)	Si2−N2−Si3	129.6(2)
Si3−N3−Si4	136.5(2)	Si3−N3−Si4	134.2(2)
Si4−N4−Si1	130.9(2)	Si4−N4−Si1	130.6(2)
N4−Si1−N1	113.4(2)	N4−Si1−N1	113.99(13)
N1−Si2−N2	114.2(2)	N1−Si2−N2	115.29(13)
N2−Si3−N3	112.7(2)	N2−Si3−N3	112.62(13)
N3−Si4−N4	113.3(2)	N3−Si4−N4	113.13(13)

nation of THF in **4** is consistent with the higher polarizability of the heavier alkali metals, only a few other structures of sodium and potassium organometallic compounds revealing this type of ligand coordination are known.[13b,18] Examples in organolithium chemistry, however, are comparatively rare in view of the vast number of structurally characterized lithium organic species.[19]

X-ray Structure of $[Cs_2(Me_2SiN(H)Me_2SiN)_2 \cdot 3THF]_\infty$ (5). Polymeric chains are characteristic features of **5** (Figure 5), as well, which emphasizes the close relation between rubidium and cesium. In contrast to the association of cations and anions in a straight line, however, a zigzag is formed in **5** with the axis of the polymer corresponding to a crystallographic 2-fold screw axis. Furthermore, the monomeric units are connected via Cs-N contacts, only, while THF ligands in addition contribute to the polymeric affiliation in **4**. Selected geometrical parameters are listed in Table 1.

Like in **4**, two different cation environments are present in **5**: terminally arranged cesium atoms (Cs2) generating the polymeric chain and multihapto-bonded cesium (Cs1) positioned almost centrally above the eight-membered silazane ring (deviation from the averaged ring center being 0.059 Å, corresponding to 2.8% of the average ring radius). It appears that further coordination of Cs1 should be possible as a THF molecule should fit into the gap between Cs1 and the adjoined monomeric unit. In fact, the transition of the zigzag into a straight chain analogous to **4** may be accomplished by introducing a THF ligand into this position bridging Cs1 and Cs2 of the associated fragment. Instead, electrostatic interaction between Cs1 and the deprotonated nitrogen atom of the neighboring silazane ring seems to be involved in the chain folding despite the large distance of 3.95 Å. For comparison, the sum of the van der Waals radii of nitrogen and cesium is 4.16 Å[16] while the covalent radii add up to only 3.05 Å[16] which is close to the range of the Cs2−N distances in **5** (3.133(3) and 3.076(2) Å). In analogy to the coordination of Rb1 in **4**, two short (Cs1−N1 = 3.207(3), Cs1−N3 = 3.125(3) Å) and two long (Cs1−N2 = 3.351(3), Cs1−N4 = 3.393(3) Å) cesium−nitrogen contacts are formed by Cs1 within the monomeric components (Figure 6). Likewise, short and long endocyclic bonds characterize the silazane ring skeleton ranging from 1.660(3) to 1.669(3) Å for the deprotonated, and from 1.747(3) to 1.756(3) Å for the N(H) functional

(18) (a) Hu, N.; Gong, L.; Jin, Z.; Chen, W. *J. Organomet. Chem.* **1988**, *352*, 61. (b) Shen, Q.; Qi, M.; Lin, Y. *J. Organomet. Chem.* **1990**, *399*, 247. (c) Brooker, S.; Edelmann, F. T.; Kottke, T.; Roesky, H. W.; Sheldrick, G. M.; Stalke, D.; Whitmire, K. H. *J. Chem. Soc., Chem. Commun.* **1991**, 144. (d) Fermin, M. C.; Ho, J.; Stephan, D. W. *J. Am. Chem. Soc.* **1994**, *116*, 6033.

(19) (a) Tatsumi, K.; Inoue, Y.; Kawaguchi, H.; Kohsaka, M.; Nakamura, A.; Cramer, R. E.; VanDoorne, W.; Taogoshi, G. J.; Richman, P. N. *Organometallics* **1993**, *12*, 352. (b) Zhang, H.; Wang, Y.; Saxena, A. K.; Oki, A. R.; Maguire, J. A.; Hosmane, N. S. *Organometallics* **1993**, *12*, 3933. (c) Boche, G.; Boie, C.; Bosold, F.; Harms, K.; Marsch, M. *Angew. Chem.* **1994**, *106*, 90; *Angew. Chem., Int. Ed. Engl.* **1994**, *33*, 115. (d) Clegg, W.; Horsburgh, L.; Mackenzie, F. M.; Mulvey, R. E. *J. Chem. Soc., Chem. Commun.* **1995**, 2011.

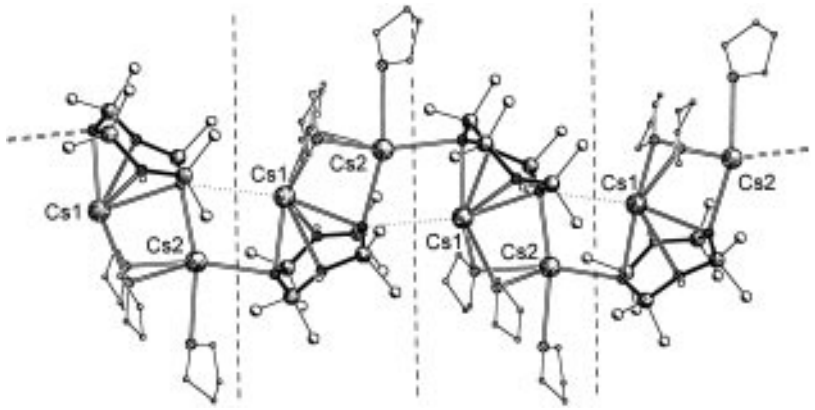

Figure 5. Polymeric structure of $[Cs_2(Me_2SiN(H)Me_2SiN)_2 \cdot 3THF]_\infty$ (**5**) in the crystal.

Table 2. Comparison of Geometrical Features of Alkali-Metalated OMCTS

	metal (structure code)				
	Li (**1**)	Na (**2**)	K (**3**)	Rb (**4**)	Cs (**5**)
degree of oligomerization	2	2	2	∞	∞
coordination number of alkali metal	3	4	5/6	4/7	5/6(7)[a]
minimal distance M—N[b] (Å)	2.156	2.455	2.838	2.957	3.125
maximal distance M—N[b] (Å)	2.879	2.902	3.112	3.161	3.393
mean deviation from av. M—N[b] (%)	10.0	6.6	3.2	2.9	3.2
average distance Si—N(H) (Å)	1.743	1.748	1.752	1.752	1.752
average distance Si—N$^-$ (Å)	1.686	1.677	1.660	1.659	1.665
Si—N bond deviation (%)	3.3	4.1	5.3	5.3	5.0
transannular N$^-$···N$^-$ distance (Å)	4.334	4.267	4.225	4.240	4.230
transannular N(H)···N(H) distance (Å)	3.541	3.739	3.836	3.811	3.849
ring distortion[c]	1.22	1.14	1.10	1.11	1.10
references	13a	13b	13b	this work	this work

[a] In parentheses, coordination number of Cs1 including the long range Cs1···N′ interaction. [b] M—N: distance of nitrogen atoms to the alkali metal positioned above the silazane ring. The minimal distance refers to M—N$^-$, the maximal distance to M—N(H). [C] ring distortion: ratio of the transannular N···N distances.

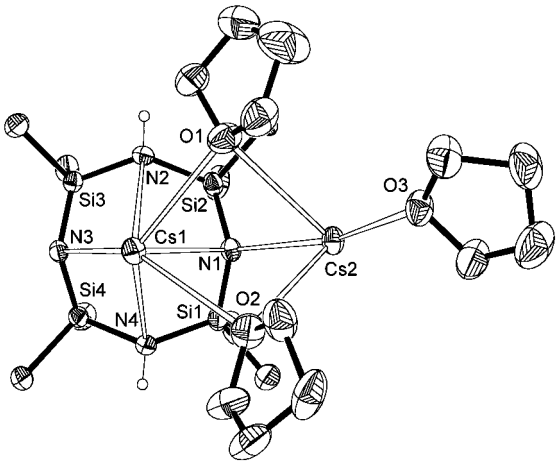

Figure 6. Asymmetric unit of **5** without H(C) atoms; anisotropic uncertainty parameters depicting 50% probability.

nitrogen atoms. The arrangement of the bridging THF molecules is somewhat different in **5** compared with **4**. Two THF ligands μ_2-bridge the same cesium atoms laterally, while in **4** each pair of rubidium atoms is bridged by only one THF molecule which is incorporated into the chain skeleton. Again, the shortest Cs—O bond is formed to the terminally coordinated THF molecule (Cs2—O3 = 3.193(2) Å); the Cs—O distances to the μ_2-bridging THF ligands range from 3.207(3) Å (Cs1—O1) to 3.379(3) Å (Cs2—O1).

Structural Comparison of Alkali-Metalated OMCTS. Table 2 summarizes selected geometrical parameters of the solid-state structures of **1**—**5**. The structural modifications induced by the variation of the alkali metal can be classified in two categories. One refers to changes in the environment of the alkali metal, the other involves the alterations in the silazane ring system. As mentioned above, the alkali metal coordination number and the degree of oligomerization correlates with the cation size. The deviation from the position centrally above the eight-membered ring decreases from lithium to cesium. A related phenomenon is apparent in several alkali metal compounds with a π-delocalized carbanionic system[20] and has been addressed as a "haptotropic effect" which depends on the relative size of the ions involved.[21] Furthermore, the different atomic radii of the alkali metals influence the angle of inclination of the terminally arranged metal atoms with respect to the silazane ring (Figure 7). The superposition of all alkali-metalated structures illustrates the increasing repulsion of the cations, although the picture is somewhat distorted due to dissimilar degrees of oligomerization as well as to the different coordination type of rubidium in **4** compared to cesium in **5**. The general tendency is nevertheless apparent. On the basis of the distances between the metal atoms a distinction into two groups is indicated which involves lithium and sodium on one hand, and potassium, rubidium, and cesium on the other hand. The similar coordination pattern of the alkali metals within these groups corre-

(20) (a) Brooks, J. J.; Rhine, W.; Stucky, G. D. *J. Am. Chem. Soc.* **1972**, *94*, 7339. (b) Zerger, R.; Rhine, W.; Stucky, G. D. *J. Am. Chem. Soc.* **1974**, *96*, 5441. (c) Hoffmann, D.; Hampel, F.; Schleyer, P. v. R. *J. Organomet. Chem.* **1993**, *456*, 13.

(21) Jemmis, E. D.; Schleyer, P. v. R. *J. Am. Chem. Soc.* **1982**, *104*, 4781.

Table 3. Crystal Data of 4 and 5

	4	5
formula	$C_{20}H_{50}Rb_2N_4O_3Si_4$	$C_{20}H_{50}Cs_2N_4O_3Si_4$
fw	677.94	772.82
crystal size (mm^3)	0.5 × 0.3 × 0.2	0.4 × 0.3 × 0.3
space group	$P\bar{1}$	$P2_1/n$
a (Å)	11.340(10)	14.4973(13)
b (Å)	11.840(10)	13.882(2)
c (Å)	14.113(13)	17.448(2)
α (deg)	70.95(5)	90
β (deg)	84.62(5)	106.799(9)
γ (deg)	67.59(4)	90
V ($Å^3$)	1655(3)	3361.5(7)
Z	2	4
temp *T* (K)	123(2)	153(2)
ρ_{calc} ($mg\ m^{-3}$)	1.360	1.527
μ (mm^{-1})	3.127	2.337
absorption correction	semiempirical[a]	semiempirical[a]
maximal transmission	0.926	0.958
minimal transmission	0.682	0.906
F(000)	704	1552
2*θ* range (deg)	8−45	8−50
no. of reflections collected	4170	7138
no. of unique reflections (R_{int})	3642 (0.020)	5806 (0.040)
no. of restraints	70	2
refined parameters	325	304
R1[b] [$I > 2\sigma(I)$]	0.034	0.023
wR2[b] (all data)	0.089	0.063
*g*1; *g*2[c]	0.0432; 3.5555	0.0198; 5.7022
largest diff. peak/hole (e $Å^{-3}$)	0.510/−0.456	0.479/−0.394

[a] From *ψ*-scans. [b] $R1 = \sum||F_o| - |F_c||/\sum|F_o|$; $wR2 = \{\sum[w(F_o^2 - F_c^2)^2]/\sum[w(F_o^2)^2]\}^{1/2}$. [c] $w = 1/[\sigma^2(F_o^2) + (g1*P)^2 + g2*P]$; $P = (F_o^2 + 2F_c^2)/3$.

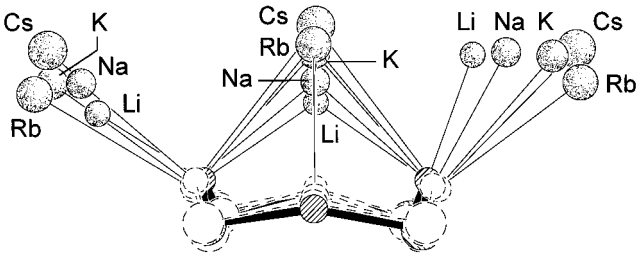

Figure 7. Superposition of all THF-solvated structures of alkali-metalated OMCTS. (THF ligands and methyl substituents have been omitted for clarity.)

sponds well with the cation radii. Lithium (0.60 Å) and sodium (0.95 Å) have similar radii, as have potassium (1.33 Å), rubidium (1.48 Å) and cesium (1.69 Å).[15] A variety of structural examples illustrate this relation[22] as in the case of the simplest organometallic compounds, alkali-metalated methane.[6] Minor inconsistencies of the structural parameters of the cesium compound within the group of the heavier alkali metal structures parallel the course of natural charges of the cation in alkali metal amides derived from *ab initio* MO calculations.[23]

The variation of the alkali metal not only influences the environment of the respective cation but also affects the geometry of the anionic moiety (Table 2). Two general tendencies can be distinguished, both of which show a consistent course. First, the discrepancy between the short Si−N$^-$ and the long Si−N(H) bonds is more pronounced in the structures of the heavier alkali metals. Second, the ring distortion which is expressed by the ratio of the transannular N···N′ distances decreases as the cation radius increases, i.e., the silazane ring approaches the symmetric crown conformation. As mentioned earlier, type and length of the Si−N bond are correlated to the effect that a shorter distance results when the bond becomes more ionic. This in turn is the case when the ionic character of the metal−amide bond increases. The charge-localizing effect of the alkali metal and, in connection with this, the cation radius are decisive factors to be considered in multihapto-bonded systems. While small cations preferably form contacts to the centers of highest negative charge, the larger and "softer" alkali cations are less charge localizing and hence coordinate to less negatively charged positions of the anionic fragment, as well. As a result, the N(H) functional and the deprotonated nitrogen atoms are almost equally attractive for an electrostatic interaction with the heavier alkali metals as revealed by the increasing similarity of the four metal−nitrogen distances (M−N distances in Table 2). At the same time, the contraction of the silazane ring along N1···N3 (which facilitates the interaction between the negatively charged nitrogen atoms and the alkali metal) becomes less important, and the distortion of the ring symmetry decreases.

Conclusion

The overall structural comparison of alkali-metalated OMCTS illustrates the close relation between lithium and sodium on one hand, and potassium, rubidium, and cesium on the other hand. The choice of the metal not only affects the environment of the cation but also induces electronic and geometrical alterations within the anion. Both can well be correlated with the differences in size and electronegativity of the alkali metal. Some unexpected inconsistencies within the course of structural and chemical characterization reveal that properties of a certain species are not yet entirely deducible from respective data of the homologous com-

(22) (a) Setzer, W. N.; Schleyer, P. v. R. *Adv. Organomet. Chem.* **1985**, *24*, 353. (b) Schade, C.; Schleyer, P. v. R. *Adv. Organomet. Chem.* **1987**, 27, 169.

(23) Lambert, C.; Kaupp, M.; Schleyer, P. v. R. *Organometallics* **1993**, *12*, 853.

pounds. This refers, for instance, to the degree of aggregation of the potassium compound and to the inactivity of elementary cesium toward OMCTS. In particular, the, at first glance incomprehensible, observation that rubidium and cesium do not react spontaneously clearly demonstrates that structural considerations have to be taken into account when estimating the reactivity of a specific system.

Experimental Section

All manipulations were carried out under an argon atmosphere using standard Schlenk techniques. Solvents were dried over Na/K alloy and freshly distilled prior to use. Octamethylcyclotetrasilazane was prepared following the procedure described in the literature.[24] ^{1}H, ^{13}C, ^{29}Si, and ^{133}Cs spectra were obtained with a Bruker AM250 and MSL400 spectrometer. All NMR spectra were recorded in THF-d_8 at room temperature from 5−10% and 20% (^{29}Si) solutions with $SiMe_4$, and CsF as external standards. Due to the high sensitivity of **4** and **5** toward oxygen and moisture, an accurate elemental analysis could not be obtained.

$[Rb_2(Me_2SiN(H)Me_2SiN)_2 \cdot 3THF]_\infty$ (4). To 1 g (11.7 mmol) of elemental rubidium in a mixture of 50 mL of THF and 50 mL of toluene was added 1.7 g (5.85 mmol) of OMCTS in 10 mL of toluene at room temperature. The rubidium metal was then activated using an ultrasonic bath (Bandelin Sonorex TK 52H) while the reaction mixture was constantly stirred under reflux, employing a mechanical disintegrater (IKA Ultra-Turrax T25). Within 3 days the metal had completely reacted and a pale yellow solution containing a small amount of a brown precipitate had formed. After filtration and maintaining the clear solution at −20 °C for 3 days small colorless blocks suitable for X-ray structure analysis formed. Yield: 2.8 g (71%), first batch. Mp: 205 °C decomposition. ^{1}H NMR in ppm: δ −0.13 (b, CH_3). ^{13}C NMR in ppm: δ +8.2, +6.6, +4.8 (m, CH_3; signals are due to different oligomeric species). ^{29}Si NMR in ppm: δ −26.3, −28.3, −34.2 (s; signals refer to different oligomeric species).

$[Cs_2(Me_2SiN(H)Me_2SiN)_2 \cdot 3THF]_\infty$ (5). Elementary cesium (1 g, 7.5 mmol) in a solution of 1.1 g (3.75 mmol) of OMCTS in 25 mL of THF was activated for 1 h at room temperature using an ultrasonic bath. The deprotonation reaction was started by adding dropwise 0.5 mL of toluene under stirring at 40 °C. After the metal was consumed completely (∼1 h) the volume of the reaction mixture was reduced to 10 mL. Subsequently, hexane was added to the solution until clouding. By addition of few drops of THF a clear, saturated solution was obtained from which colorless blocks crystallized upon cooling at −20 °C over 4 days. Yield: 2.5 g (86%), first batch. Mp: 320 °C decomposition. ^{1}H NMR in ppm: δ −0.14 (s, CH_3). ^{13}C NMR in ppm: δ +8.7 (s, CH_3; $^{1}J_{C-Si}$ 57 Hz). ^{29}Si NMR in ppm: δ −32.0 (s; $^{1}J_{Si-C}$ 57 Hz). ^{133}Cs NMR in ppm: δ +148.9 (s).

X-ray Measurements of 4 and 5. The crystal data for both structures are presented in Table 3. The data were collected at low temperatures using an oil-coated shock-cooled crystal[25] on a Stoe-Siemens AED (**4**) and Stoe-Siemens-Huber (**5**) four-circle diffractometer with Mo Kα (λ = 0.71073 Å) radiation. The structures were solved by direct methods (SHELXS-90[26]) and refined by least-squares iteration on F^2 (SHELXL-93[27]) employing all data, with a weighting scheme of $w = 1/[\sigma^2(F_o^2) + (g1P)^2 + g2P]$ with $P = (F_o^2 + 2F_c^2)/3$. All non-hydrogen atoms were refined anisotropically. The H(N) atoms were located by difference Fourier synthesis and refined isotropically with the displacement parameters constrained to equal 1.2 U(equivalent) of the attached nitrogen atom and the N−H distance restrained to approximate 88 pm. All other hydrogen atoms were geometrically positioned and treated riding. Similarity restraints were applied to geometrically equivalent bond lengths and angles of the THF ligands. A disorder in one THF molecule of **4** was resolved and refined to 38.4/61.6% site occupation employing ADP restraints.

Acknowledgment. The authors thank the Deutsche Forschungsgemeinschaft, the Fonds der Chemischen Industrie, and the Volkswagen Stiftung for financial support.

Supporting Information Available: Tables of crystal data, fractional coordinates, bond lengths and angles, anisotropic displacement parameters, and hydrogen atom coordinates (22 pages). Ordering information is given on any current masthead page.

OM960434W

(24) Brewer, S. D.; Haber, C. P. *J. Am. Chem. Soc.* **1948**, *70*, 3888.
(25) Kottke, T.; Stalke, D. *J. Appl. Crystallogr.* **1993**, *26*, 615.
(26) Sheldrick, G. M. *Acta Crystallogr., Sect. A* **1990**, *46*, 467.
(27) Sheldrick, G. M. SHELXL-93 program for crystal structure refinement, University of Göttingen, 1993.